Published in final edited form as:
Cancer Res. 2012 October 1; 72(19): 5111–5118. doi:10.1158/0008-5472.CAN-12-0624.

CD133+ Melanoma Subpopulations Contribute to Perivascular Niche Morphogenesis and Tumorigenicity through Vasculogenic Mimicry

Chiou-Yan Lai[1], **Brian E. Schwartz**[2], and **Mei-Yu Hsu**[1,2,*]

[1]Program in Dermatopathology, Department of Pathology, Brigham and Women's Hospital, Harvard Medical School, Boston, MA 02115

[2]Department of Dermatology, Boston University Medical Center, Boston, MA 02118

Abstract

Tumor cell subpopulations that express cancer stem cell markers such as CD133 (prominin1) or ABCB5 are thought to be crucial for tumor initiation and heterogeneity, but their biological significance in melanoma has been controversial. Here, we report that $CD133^+$ and $ABCB5^+$ subpopulations are co-localized in melanomas in perivascular niches that contain CD144 (VE-cadherin)$^+$ melanoma cells forming vessel-like channels, a phenomenon termed vasculogenic mimicry (VM). RNAi-mediated attenuation of CD133 established its critical function in morphogenesis of these perivascular niches as well as in melanoma tumorigenicity. Niche-associated genes CD144 and ABCB5 were downregulated in tumors derived from CD133 knockdown (KD) melanoma cells, compared to controls. CD133KD cells also lacked the ability to form $CD144^+$ VM-like channels in a manner that was associated with a depletion of the $ABCB5^+$ cell subpopulation. Lastly, CD133 KD cells exhibited poorer tumor growth *in vivo*. Taken together, our findings corroborate models in which $CD133^+/ABCB5^+$ melanoma cells reside in a complex anastomosing microvascular niche that encompasses $CD144^+$ VM channels as well as authentic endothelial cell-lined blood vessels. Further, they indicate that $CD133^+$ cells act as stem-like cells, which drive tumor growth by promoting VM and the morphogenesis of a specialized perivascular niche in melanoma.

Keywords

CD133; melanoma; cancer stem cells; niche; vasculogenic mimicry

Introduction

Melanoma is one of the most virulent human cancers due to its tendency to metastasize and resistance to conventional anti-cancer therapies. One key factor responsible for treatment failure relates to tumor heterogeneity, particularly the cell populations possessing stem cell-like properties (1). Several putative stem cell markers have been reported in melanoma to date (2–9). Among these, CD133 (human prominin 1), a transmembrane pentaspan glycoprotein found in stem and early progenitor cells of varying histogenesis, and ABCB5, an ATP-binding cassette (ABC) efflux transporter responsible for melanoma chemoresistance, are the best characterized. Monzani et al (5) demonstrated that human

*Corresponding author: Department of Dermatology, Boston University Medical Center, 609 Albany St., J-410, Boston, MA 02118. Phone: 617-638-5557; Fax: 617-638-5515; meiyuhsu@bu.edu.

Disclosure of Potential Conflict of Interest: No potential conflicts of interest were disclosed.

melanoma samples contain $CD133^+$ fractions, which confer multi-potent differentiation *in vitro*, as well as tumorigenic growth *in vivo*. CD133 downregulation in melanoma cells led to reduced motility and metastasis (10). Frank et al (2) reported that $ABCB5^+$ melanoma cells co-express CD133 *in vitro* and exhibit self-renewal, differentiation and tumor-initiating capacities *in vivo*. Furthermore, direct targeting of the $ABCB5^+$ melanoma subpopulation using a monoclonal antibody (mAb) resulted in Ab-dependent cell-mediated cytotoxicity exerting tumor-inhibiting effects (3). Findings from these earlier studies are in keeping with the traditional "hierarchical model" of cancer stem cell (CSC) hypothesis, where the marker-expressing fractions are endowed with self-renewal capacity and sufficient to reconstitute/repopulate the tumor by generating both progenitor marker-positive daughter CSC and marker-negative differentiated progenies through asymmetrical division. However, the recent identification of tumor-initiating potential within $CD133^-$ subsets in brain, colon, and lung cancers as well as melanoma raises questions on the biological relevance of these putative marker-expressing subsets (11–14).

Although traditionally CSC are defined mainly by their ability to self-renew and differentiate, mounting evidence now suggests that like normal stem cells, CSC reside in specialized compartments, known as the "niche", which provide the essential cues for cell fate determination (15–17). For example, a recent report by Calabrese et al (18) localized brain tumor initiating cells (BTIC) to the perivascular microenvironment, the so-called "perivascular niches". Disruption of such vascular "niches" ablates the brain tumor initiating population, resulting in growth arrest (18). Rather than passively, functionally depend on the supporting blood vessels within the "niche", it is now clear that the BTIC actively and directly participate in tumor vascularization through transendothelial differentiation (19, 20). Despite advances in identifying markers for melanoma-initiating cells (MIC) and subsequent characterization of different MIC subsets, their microenvironmental "niches" have not been defined.

To test the biological significance of $CD133^+$ melanoma subsets, we: 1) examined the expression of $CD133^+$ subsets *in vitro* and *in vivo*, 2) characterized their microenvironmental "niches" in the context of tumor microcirculation, comprised of not only authentic blood vessels but also VM channels formed by transdifferentiated melanoma cells (21–23), and 3) explored their functional role with regard to tumor growth and "niche" maintenance through loss-of-function analysis using lentiviral shRNA. Defining and characterizing the MIC "niche" and molecular mechanisms through which different resident cell types communicate offers a novel opportunity to therapeutically eliminate MIC directly or indirectly by targeting the stromal co-dependence.

Materials and Methods

Cell Culture

Isogenic melanoma cell lines derived from different disease stages of tumor progression (obtained from Dr. M. Herlyn at the Wistar Institute, Philadelphia, PA) were cultured as previously described (24). These were comprised of primary vertical growth phase (VGP) melanoma cell lines WM115 and WM983A, and their metastatic counterparts WM239A and WM983C, respectively, and metastatic melanoma variants, WM164, WM1617, 1205Lu, and SK-MEL-5. Metastatic melanoma cell lines A375 and its highly invasive variant, A375 P-5 (25) (obtained from Dr. M.J.C. Hendrix at the Northwestern University, Chicago, IL) were maintained as previously described (25). All cell lines were tested using the PowerPlex 18D system (Promega BioSciences, San Luis Obispo, CA).

Flow Cytometry

Surface CD133 expression on melanoma cells was analyzed by flow cytometry using phycoerythrin (PE)-conjugated CD133/1 clone AC133 antibody (Miltenyi Biotec, Gladbach, Germany). PE-conjugated isotype control mAb (Abcam, Cambridge, MA) served as a control. 7AAD (MP Biomedicals, Solon, OH) was added to samples prior to flow analysis to facilitate discrimination against dead cells. The expression profile was analyzed with acquisition of fluorescence emission at the FL2 (PE) spectrum on LSR II (BD Biosciences, San Jose, CA) using FACSDiva software (BD Biosciences).

Immunohistochemistry

Dewaxed formalin-fixed and paraffin-embedded (FFPE) melanoma tissue sections were subjected to antigen-retrieval using a Pascal pressure chamber (Dako, Carpinteria, CA) followed by immunohistochemical staining using rabbit anti-CD133 (Abcam), goat anti-ABCB5 (Abcam), or isotype-matched negative control primary antibodies (Abcam), and peroxidase-conjugated goat anti-rabbit or horse anti-goat secondary antibodies (Vector Laboratories, Burlingame, CA). Immunoreactivity was visualized by NovaRed peroxidase substrate (Vector Laboratories).

Patient Tissue Samples

Decoded patient samples, including 7 benign nevi, 7 primary cutaneous melanomas (ranging from Clark level III–IV), and 7 metastatic melanomas (from various tissue sites, such as lung, lymph node, and cutaneous metastases), were obtained from the archive at the Department of Pathology, Brigham and Women's Hospital according to Institutional Review Board (IRB)-approved protocol (#2009P001579). No prior treatment history of these individuals was available.

Immunofluorescence

Frozen melanoma xenograft sections or dewaxed FFPE patient tissue sections following antigen retrieval were subjected to double indirect immunofluorescence using standard procedures. The primary antibodies used in this study are rabbit anti-hCD144 (human-specific; Cell Signaling Technology, Danvers, MA), rabbit anti-CD144 (reactive to human and mouse, Abcam), goat anti-GFP (Novus Biologicals, Littleton, CO), rabbit anti-CD133 (Abcam), rat anti-mouse CD31 (BD Biosciences), mouse anti-β3 integrin (SAP; gift from Dr. M. Herlyn), and mouse anti-high molecular weight proteoglycans (ME31.3; gift from Dr. M. Herlyn). The secondary antibodies employed are FITC-conjugated donkey anti-rabbit IgG (Accurate Chemical & Scientific Corporation, Westbury, NY), FITC-conjugated donkey anti-goat (Jackson Immunoresearch, West Grove, PA), AlexaFluor 594-conjugated donkey anti-rabbit, AlexaFluor 594-conjugated donkey anti-rat IgG, and AlexaFluor 488-conjugated goat anti-mouse IgG_1 (Invitrogen, Grand Island, NY) antibodies. Isotype-matched rabbit, goat, or rat immunoglobulin was used in place of the primary antibody for control. Sections were mounted with Vectashield containing DAPI (Vector Laboratories) and inspected under a BX51/BX52 fluorescence microscope (Olympus, Melville, NY) or DSU confocal microscope (Olympus).

In Situ Hybridization

In situ hybridization was performed as previously described (26). The sequences used for human CD133 probes are listed as follows: CD133 sense strand 5′-GACCCAAGACTCCCATAAAGC-3′; CD133 antisense strand 5′-GCAGCCCCAGGACACAGCATA-3′. The ABCB5 probes were previously described (27). The probes were labeled with digoxigenin using DIG RNA labeling kit (Roche, Indianapolis, IN).

CD133 Knockdown in Melanoma Cells by Lentiviral shRNA

Lentiviral vectors were generated by co-transfecting pLKO.1-CD133 (Sigma, St. Louis, MO), containing shRNA against human CD133, or non-target control shRNA (Sigma) with packing plasmids VSVg and pCMV-ΔR8.2 (Sigma) into 293T packing cells using Lipofectamine 2000 (Invitrogen) according to the manufacturer's protocol. Lentiviral supernatants were used to infect WM1617 melanoma cells. Stable transfectants were selected with 1 μg/ml puromycin for a period of 7 days.

Western Blotting

Cell lysates and xenograft tissue homogenates were extracted in lysis buffer and quantified by a BCA protein assay kit (Pierce, Rockford, IL) as previously described (28). Bovine aortic endothelial cell (BAEC, Cell Signaling Technology) and A375 lysates were included as a positive control for CD144 and ABCB5, respectively. Equal amounts (10–50 μg) of protein were subjected to electrophoresis, followed by probing with rabbit anti-CD133 (Abcam; Western blot for cell lysates) at 1 μg/ml or mouse anti-CD133 (Miltenyi Biotec, clone W6B3C1; Western blot for xenograft homogenates) at 1:200; rabbit anti-CD144 (Cell Signaling Technology) at 1:1000; rabbit anti-ABCB5 (Abgent, San Diego, CA) at 1:100; and mouse anti-beta actin (Abcam) at 1:5000. Immunoreactive bands were visualized by SuperSignal West Pico Chemiluminescent Substrate (Pierce, Rockford, IL). Densitometry measurements were performed using Image J software (National Institutes of Health, Bethesda, MD), where beta-actin served as a loading control.

Melanoma Xenografts

For characterization of the perivascular "niche", 3×10^6 A375, A375GFP (A375 stably expressing GFP mediated by lentiviral gene transfer), SK-MEL-5, and WM1617 melanoma cells were injected subcutaneously in the dorsal skin of each SCID mouse (CB17; Taconic Laboratory, Germantown, NY). Melanoma xenografts were harvested when tumors reach 1 cm^3, and subjected to histopathologic analysis.

In Vivo Tumorigenicity

For the effect of CD133 silencing on tumorigenicity, 2×10^5 WM1617 melanoma cells infected by control and CD133 shRNA lentiviral constructs were injected subcutaneously in the dorsal skin of each SCID mouse (CB17; Taconic Laboratory; 5 mice per condition). In another separate experiment, 3×10^6 control and CD133 KD WM1617 melanoma cells were injected per mouse (7 mice per condition) to ensure the generation of sizable CD133 KD xenografts for various analyses, including immunohistochemistry, immunofluorescence, and real-time quantitative RT-PCR as described above. Tumor volume was monitored and determined as the volume of ellipsoid: 4/3 π (width/2 × length/2 × height/2). Statistical analyses were performed using ANOVA following log transformation.

Real-Time Quantitative RT-PCR (qRT-PCR)

RNA from frozen tumors was extracted and reverse transcribed into cDNA using μMACS™ One-step cDNA kit (Miltenyi Biotec) according to the manufacturer's instructions. Real-time quantitative PCR (q-PCR) was subsequently performed on a 7300 Real-Time PCR System (Applied Biosystems, Foster City, CA) using human-specific primers, CD133 (Hs00195682_m1), ABCB5 (Hs00698751_m1), or CD144 (Hs00174344_m1). All samples were run in triplicate. The actin housekeeping gene was used for normalization and data analyzed using $2^{-\Delta\Delta Ct}$ method (29).

Results

CD133 Expression in Melanoma Correlates with Tumor Progression *In Vivo*

Using flow cytometry, we identified $CD133^+$ fractions in seven melanoma cell lines, including WM164, WM1617, A375P-5, and two isogenic cell pairs: WM115 (VGP)/WM239A (Met) and WM983A (VGP)/WM983C (Met), out of a total of nine (7/9) *in vitro*. The $CD133^+$ subsets in the positive cell lines range from 0.2% to 76.3% (Figure 1A). Two metastatic melanoma cell lines 1205Lu and A375 exhibited no detectable CD133. CD133 expression in patient samples was also examined by immunofluorescence (IF). Seven lesions each of different stages of melanoma progression, including ordinary nevi, primary melanomas, and metastatic melanomas, were analyzed. We found that the average percentage of the $CD133^+$ fraction rising stepwise from 0% in nevi to ~2% in metastatic lesions, while the percentage of samples containing the $CD133^+$ fraction increasing from 0/7 in nevi to 7/7 in metastatic lesions, indicating that the $CD133^+$ subset is more prevalent as the disease progresses (Figure 1B). To validate that the $CD133^+$ cells identified in the patient samples were indeed melanoma cells, double IF was employed using antibodies directed to melanoma-associated antigens (MAA), such as β3 integrin subunit or high molecular weight proteoglycans (Figure 1C). Taken together, CD133 expression correlates with tumor progression *in vivo*, though no obvious correlation with tumor progression was observed *in vitro* since CD133 expression was detected in both primary melanoma cell lines (2/2; e.g., WM115 and WM983A) but not in all metastatic melanoma cell lines screened (5/7).

$CD133^+$/$ABCB5^+$ Subsets Coincide with $CD144^+$ Areas of VM: the "Perivascular Niche"

To explore the tissue distribution of $CD133^+$ subsets in melanoma, we conducted immunohistochemistry (IHC) and *in situ hybridization* (ISH) in melanoma xenografts derived from WM1617 (not shown), A375 (Figure 2), and SK-MEL-5 melanoma cells (not shown). We found that $CD133^+$ fractions coincide with $ABCB5^+$ subsets, and are arranged in a branching network pattern identical to the PAS^+ VM channels (Figure 2A). To further characterize VM *in vivo*, we analyzed the tumor vasculatures in relationship to the $CD133^+$ subsets in GFP-labeled A375 melanoma xenografts by multilabel IF. Using CD144 as a marker for VM, we identified circulatory networks comprised of $CD144^+$/GFP^+ melanoma cell-lined VM channels, $CD144^+$/GFP^- endothelial cell (EC)-lined mouse blood vessels (BV), and mosaic vessels (MV) partially lined by both $CD144^+$/GFP^+ channel-forming melanoma cells and $CD144^+$/GFP^- mouse ECs (Figure 2B). Interestingly, $CD144^+$ VM-engaging melanoma cells (Figure 2C, right panel) are confined in areas in close proximity to $CD31^+$ mouse BV (Figure 2C, left panel) in consecutive tissue sections. Furthermore, IF localizes $CD133^+$ subsets (Figure 2D, left panel) to $CD144^+$ VM fractions (Figure 2D, right panel) intimately associated with $CD31^+$ mouse BV in a "perivascular pattern". Collectively, these data suggest that $CD133^+$/$ABCB5^+$ subsets reside in a complex anastomosing microvascular "niche" encompassing $CD144^+$ melanoma cell-lined VM channels, mosaic vessels partially lined by $CD144^+$ VM-engaging melanoma cells and endothelial cells, and authentic blood vessels.

CD133 Silencing in Melanoma by Lentiviral shRNA

To elucidate the functional role for CD133, we generated stable CD133 KD in WM1617 melanoma cells using lentiviral shRNA. Western blotting revealed over 90% knockdown efficiency at the protein level achieved by CD133 shRNA both *in vitro* and *in vivo* (xenografts) compared to the control harboring non-target shRNA. IHC (Figure 3B) further verified downregulation of CD133 *in vivo*, as only the non-target control but not CD133 KD xenografts retained the "perivascular niche" VM-like pattern of CD133 expression.

CD133 KD Downregulates CD144 and ABCB5, Attenuates VM-like Melanoma Channel Formation, and Retards Tumor Growth

When we analyzed CD133 KD xenografts by real-time qRT-PCR using human-specific primers, expression profiling showed concurrent downregulation of CD144 and ABCB5 in CD133 KD xenografts compared to their non-target control counterparts (Figure 4A). IF staining revealed that CD133 KD xenografts exhibited attenuated $CD144^+$ VM-like melanoma channel formation, whereas the control xenografts retained $CD144^+$ VM channels in close association with $CD31^+$ authentic blood vessels (Figure 4B). IHC analysis (Figure 4C) also confirmed the depletion of vascular "niche"-associated $ABCB5^+$ subsets in CD133 KD xenografts. Attempts to further validate CD144 downregulation in CD133 KD xenografts using Western blotting (BAEC lysate included as a positive control) were unsuccessful due to sensitivity issues given the minute fraction of the $CD144^+$ subset (Figure 4D, top panel; note that CD144 signals were undetectable both in the control and KD xenografts despite maximal loading and prolonged overnight exposure). Western blotting (Figure 4D, middle panel; using A375 cell lysate as a positive control); however, confirmed downregulation of ABCB5 at the protein level in CD133 KD xenografts. Furthermore, in two separate tumorigenicity assays, CD133 KD significantly ($p< 0.05$) retarded tumor growth compared to the non-target control *in vivo* (Figure 4E), while in conventional monolayer growth as well as soft agar assays, both CD133 KD and control cells exhibited comparable growth rates and clonogenicity *in vitro* (Supplemental Figure 1).

Discussion

The recognition of cancers as heterogeneous at both the genomic and cellular levels has prompted intense investigation of cancer cell subpopulations. Of particular interest are the subpopulations that exhibit stem cell-like properties, since these may be recalcitrant to traditional cancer therapies, and therefore, contribute to tumor recurrence and metastasis. Although potential cancer cell populations expressing stem cell-like biomarkers in melanoma are studied extensively (2–8, 30), the microenvironment that supports their functional integrity has received scant attention. Our data reveal that $CD133^+/ABCB5^+$ subpopulations coincide with fractions of $CD144^+$ melanoma cells forming VM-like channels, where high-density EC-lined blood vessels also reside (Figure 2). Parallel to our findings, Frank et al (27) recently reported that the $ABCB5^+$ melanoma fractions preferentially express VM markers, CD144 and Tie-1. Furthermore, increasing evidence now supports the notion that stem cell marker-expressing tumor subpopulations are closely associated with VM. For example, stem cell marker CD271 is preferentially expressed by the VM-forming uveal melanoma cells (31), and the $CD133^+$ subset of triple-negative breast cancer correlates with VM-forming capability (32).

The close spatial association between $CD133^+/ABCB5^+$ subsets and the blood vessels is reminiscent of the "perivascular niche" concept of BTIC, where the tumor vasculature serves as a privileged environment that provides the cues to preserve the functional integrity of BTIC. However, the flow of signals within the "niche" is not unidirectional. Compelling evidence now indicates that complex reciprocal and coordinated communications exist between the BTIC and the perivascular "niche" (15, 33, 34). For example, BTIC-associated factors, such as VEGF (19, 20, 35) and CXCL12 or stromal derived factor-1 (SDF-1) (36) have been shown to contribute to the formation of vascular "niches" through paracrine stimulation of endothelial cells. In addition, several laboratories have recently demonstrated that BTIC are also able to contribute directly to vascular "niche" through transdifferentiating towards endothelial cell lineage. In this regard, BTIC-derived $CD31^+$ ECs were found to incorporate into the tumor vasculature as demonstrated by fluorescent lineage tracer and identification of cancer cell-specific molecular signatures (20, 35, 37). Parallel to this, we observe that the melanoma vascular "niche" encompasses a complex vascular network

consisting not only of authentic EC-lined blood vessels, but also of VM channels formed by $CD144^+$ transdifferentiated melanoma cells and mosaic vessels (Figure 2B). Interestingly, unlike BTIC-derived ECs, the $CD144^+$ VM-engaging melanoma cells do not express the conventional EC marker, CD31. Nevertheless, the plasticity of tumor cells to differentiate toward endothelial lineage is strikingly similar (21, 22).

Although the role of CD133 as a cancer stem cell marker is supported by multipotency *in vitro* and tumorigenicity *in vivo* in various human cancers, tumor-initiating potentials within $CD133^-$ fractions have been reported in brain, colon, and lung cancers (11–14) as well as in melanoma (38). In this study, we found that A375 melanoma cells, despite harboring a comparable number of $CD133^+$ cells in xenografts (Figure 2), are negative for CD133 *in vitro* (Figure 1A). Similar induction of $CD133^+$ subsets from $CD133^-$ cells *in vivo* have been observed by others (9, 13), suggesting that tumor "stemness" is a dynamic process and progenitor marker-negative cells may evolve into cancer stem cells through proper environment cues or accumulating genetic alterations, the so-called "stochastic" model of cancer stem cell hypothesis (39, 40). The plasticity of "stemness" in cancer cells is further supported by recent reports where CSC-like phenotype can be induced in non-CSC in response to ectopic expression or upregulation of stem cell-associated transcription factors (41, 42). Due to the dynamic nature of the tumor "stemness", single marker-based targeting may have limited benefit and the success of cancer stem cell-targeted therapy may rely on "niche"-dependent strategies (15, 33, 43). Adding to the complexity is the notion of a modified "hierarchical" model of cancer stem cells, which postulates that several different types of cancer stem cells may exist in a given tumor, yet a subset of these are better suited to survive and proliferate in a given microenvironment. This scenario provides an explanation for the lack of complete growth inhibition in CD133 KD cells *in vivo* (Figure 4E), and again potentially be a disincentive for developing therapeutics targeting a specific class of cell surface markers (44, 45).

Although the precise cellular function of CD133 is largely unknown, downregulation of CD133 in melanoma xenografts resulted in growth retardation (Figure 4E), attenuated $CD144^+$ VM channel formation and depleted $ABCB5^+$ subsets within perivascular "niche" (Figure 4A–D), and reduced cell motility and metastasis (5), supporting its role in tumor growth and maintenance. Thus, our data suggest that $CD133^+$ subsets may contribute to perivascular niche morphogenesis and tumorigenesis through coordinating $CD144^+$ VM formation. Interestingly, CD133 KD does not appear to render growth disadvantage either in conventional monolayer culture or in soft agar *in vitro* (Supplemental Figure 1), further highlighting the biological importance of the "niche" microenvironment in the phenotypic/functional rendering of MIC subpopulations.

The underlying mechanisms through which the $CD133^+$ subsets contribute to VM in melanoma are unclear; however, several molecular pathways that regulate VM have recently been identified (46). For example, VEGF-A signaling upregulates VM-associated genes, such as CD144 and EphA2, in stem cell marker-expressing tumor populations (27, 47) and VEGFR-1 knockdown inhibits VM-forming ability of $ABCB5^+$ melanoma cells (27). Expression of pigment epithelium-derived factor (PEDF) inversely correlates with VM, and PEDF downregulation in non-aggressive melanoma cells induces the VM phenotype (48). Furthermore, inhibition of Nodal function in aggressive melanoma cells either with a functional blocking antibody (49) or via Notch4 inhibition (50) reduces their VM-engaging ability.

In summary, our work underscores the importance of understanding the relationship between the unique tumor microenvironment and cancer stem cells themselves. This is especially critical in light of the growing awareness of cancer stem cell plasticity and the

challenge of therapeutically targeting cells based solely on surface markers. Future work should focus on the specific signaling pathways responsible for the ability of the $CD133^+$/$ABCB5^+$ subset to generate VM-dependent vascular "niche", and the presumed reciprocal ability of the VM/vascular "niche" to induce the $CD133^+$ phenotype from $CD133^-$ cells. Such studies will be essential for uncovering novel therapeutic targets and may facilitate a two-pronged approach to cancer treatment that involves targeting stem cells as well as the signaling pathways responsible for inducing/sustaining them.

Supplementary Material

Refer to Web version on PubMed Central for supplementary material.

Acknowledgments

We thank Drs. M. Herlyn (Wistar Institute, Philadelphia, PA) and M.J.C. Hendrix (Northwestern University, Chicago, IL) for providing melanoma cell lines.

Grant Support

This work was supported in part by NIH grant R01-138649 and Brigham and Women's Hospital, Department of Pathology start-up fund to M-Y. H.

References

1. Wicha MS, Liu S, Dontu G. Cancer stem cells: an old idea--a paradigm shift. Cancer research. 2006; 66:1883–90. discussion 95–6. [PubMed: 16488983]
2. Frank NY, Margaryan A, Huang Y, Schatton T, Waaga-Gasser AM, Gasser M, et al. ABCB5-mediated doxorubicin transport and chemoresistance in human malignant melanoma. Cancer research. 2005; 65:4320–33. [PubMed: 15899824]
3. Schatton T, Frank MH. Cancer stem cells and human malignant melanoma. Pigment cell & melanoma research. 2008; 21:39–55. [PubMed: 18353142]
4. Fang D, Nguyen TK, Leishear K, Finko R, Kulp AN, Hotz S, et al. A tumorigenic subpopulation with stem cell properties in melanomas. Cancer research. 2005; 65:9328–37. [PubMed: 16230395]
5. Monzani E, Facchetti F, Galmozzi E, Corsini E, Benetti A, Cavazzin C, et al. Melanoma contains CD133 and ABCG2 positive cells with enhanced tumourigenic potential. Eur J Cancer. 2007; 43:935–46. [PubMed: 17320377]
6. Boiko AD, Razorenova OV, van de Rijn M, Swetter SM, Johnson DL, Ly DP, et al. Human melanoma-initiating cells express neural crest nerve growth factor receptor CD271. Nature. 2010; 466:133–7. [PubMed: 20596026]
7. Chandrasekaran S, DeLouise LA. Enriching and characterizing cancer stem cell sub-populations in the WM115 melanoma cell line. Biomaterials. 2011; 32:9316–27. [PubMed: 21917310]
8. Civenni G, Walter A, Kobert N, Mihic-Probst D, Zipser M, Belloni B, et al. Human CD271-positive melanoma stem cells associated with metastasis establish tumor heterogeneity and long-term growth. Cancer research. 2011; 71:3098–109. [PubMed: 21393506]
9. Roesch A, Fukunaga-Kalabis M, Schmidt EC, Zabierowski SE, Brafford PA, Vultur A, et al. A temporarily distinct subpopulation of slow-cycling melanoma cells is required for continuous tumor growth. Cell. 2010; 141:583–94. [PubMed: 20478252]
10. Rappa G, Fodstad O, Lorico A. The stem cell-associated antigen CD133 (Prominin-1) is a molecular therapeutic target for metastatic melanoma. Stem cells (Dayton, Ohio). 2008; 26:3008–17.
11. Joo KM, Kim SY, Jin X, Song SY, Kong DS, Lee JI, et al. Clinical and biological implications of CD133-positive and CD133-negative cells in glioblastomas. Laboratory investigation; a journal of technical methods and pathology. 2008; 88:808–15.

12. Wang J, Sakariassen PO, Tsinkalovsky O, Immervoll H, Boe SO, Svendsen A, et al. CD133 negative glioma cells form tumors in nude rats and give rise to CD133 positive cells. International journal of cancer. 2008; 122:761–8.
13. Shmelkov SV, Butler JM, Hooper AT, Hormigo A, Kushner J, Milde T, et al. CD133 expression is not restricted to stem cells, and both CD133+ and CD133-metastatic colon cancer cells initiate tumors. The Journal of clinical investigation. 2008; 118:2111–20. [PubMed: 18497886]
14. Meng X, Li M, Wang X, Wang Y, Ma D. Both CD133+ and CD133-subpopulations of A549 and H446 cells contain cancer-initiating cells. Cancer science. 2009; 100:1040–6. [PubMed: 19385971]
15. Barcellos-Hoff MH, Newcomb EW, Zagzag D, Narayana A. Therapeutic targets in malignant glioblastoma microenvironment. Seminars in radiation oncology. 2009; 19:163–70. [PubMed: 19464631]
16. Wurmser AE, Palmer TD, Gage FH. Neuroscience. Cellular interactions in the stem cell niche. Science (New York, NY. 2004; 304:1253–5.
17. Moore KA, Lemischka IR. Stem cells and their niches. Science (New York, NY. 2006; 311:1880–5.
18. Calabrese C, Poppleton H, Kocak M, Hogg TL, Fuller C, Hamner B, et al. A perivascular niche for brain tumor stem cells. Cancer cell. 2007; 11:69–82. [PubMed: 17222791]
19. Veeravagu A, Liu Z, Niu G, Chen K, Jia B, Cai W, et al. Integrin alphavbeta3-targeted radioimmunotherapy of glioblastoma multiforme. Clin Cancer Res. 2008; 14:7330–9. [PubMed: 19010848]
20. Wang R, Chadalavada K, Wilshire J, Kowalik U, Hovinga KE, Geber A, et al. Glioblastoma stem-like cells give rise to tumour endothelium. Nature. 2010; 468:829–33. [PubMed: 21102433]
21. Hendrix MJ, Seftor EA, Hess AR, Seftor RE. Vasculogenic mimicry and tumour-cell plasticity: lessons from melanoma. Nature reviews Cancer. 2003; 3:411–21.
22. Dome B, Hendrix MJ, Paku S, Tovari J, Timar J. Alternative vascularization mechanisms in cancer: Pathology and therapeutic implications. The American journal of pathology. 2007; 170:1–15. [PubMed: 17200177]
23. Demou ZN, Hendrix MJ. Microgenomics profile the endogenous angiogenic phenotype in subpopulations of aggressive melanoma. Journal of cellular biochemistry. 2008; 105:562–73. [PubMed: 18655191]
24. Hsu, MY.; Elder, DE.; Herlyn, M. The Wistar melanoma (WM) cell lines. In: Masters, J.; Palsson, B., editors. Human cell culture. Nowell: Kluwer publishers; 1999. p. 259-74.
25. Yohem KH, Seftor EA, Meyskens FL Jr, Hendrix MJ. Cloning efficiency of human melanoma cells is modulated after invasion through a reconstituted basement membrane. Cancer letters. 1989; 45:135–43. [PubMed: 2731157]
26. Zhan Q, Signoretti S, Whitaker-Menezes D, Friedman TM, Korngold R, Murphy GF. Cytokeratin15-positive basal epithelial cells targeted in graft-versus-host disease express a constitutive antiapoptotic phenotype. The Journal of investigative dermatology. 2007; 127:106–15. [PubMed: 17039241]
27. Frank NY, Schatton T, Kim S, Zhan Q, Wilson BJ, Ma J, et al. VEGFR-1 expressed by malignant melanoma-initiating cells is required for tumor growth. Cancer research. 2011; 71:1474–85. [PubMed: 21212411]
28. Hsu MY, Rovinsky SA, Lai CY, Qasem S, Liu X, How J, et al. Aggressive melanoma cells escape from BMP7-mediated autocrine growth inhibition through coordinated Noggin upregulation. Laboratory investigation; a journal of technical methods and pathology. 2008; 88:842–55.
29. Livak KJ, Schmittgen TD. Analysis of relative gene expression data using real-time quantitative PCR and the 2(-Delta Delta C(T)) Method. Methods (San Diego, Calif. 2001; 25:402–8.
30. Pietra G, Manzini C, Vitale M, Balsamo M, Ognio E, Boitano M, et al. Natural killer cells kill human melanoma cells with characteristics of cancer stem cells. International immunology. 2009; 21:793–801. [PubMed: 19491215]
31. Valyi-Nagy K, Kormos B, Ali M, Shukla D, Valyi-Nagy T. Stem cell marker CD271 is expressed by vasculogenic mimicry-forming uveal melanoma cells in three-dimensional cultures. Molecular vision. 2012; 18:588–92. [PubMed: 22419851]

32. Liu TJ, Sun BC, Zhao XL, Zhao XM, Sun T, Gu Q, et al. CD133(+) cells with cancer stem cell characteristics associates with vasculogenic mimicry in triple-negative breast cancer. Oncogene. 2012
33. Denysenko T, Gennero L, Roos MA, Melcarne A, Juenemann C, Faccani G, et al. Glioblastoma cancer stem cells: heterogeneity, microenvironment and related therapeutic strategies. Cell biochemistry and function. 2010; 28:343–51. [PubMed: 20535838]
34. Hjelmeland AB, Lathia JD, Sathornsumetee S, Rich JN. Twisted tango: brain tumor neurovascular interactions. Nature neuroscience. 2011; 14:1375–81.
35. Soda Y, Marumoto T, Friedmann-Morvinski D, Soda M, Liu F, Michiue H, et al. Transdifferentiation of glioblastoma cells into vascular endothelial cells. Proceedings of the National Academy of Sciences of the United States of America. 2011; 108:4274–80. [PubMed: 21262804]
36. Maderna E, Salmaggi A, Calatozzolo C, Limido L, Pollo B. Nestin, PDGFRbeta, CXCL12 and VEGF in glioma patients: different profiles of (pro-angiogenic) molecule expression are related with tumor grade and may provide prognostic information. Cancer biology & therapy. 2007; 6:1018–24. [PubMed: 17611402]
37. Ricci-Vitiani L, Pallini R, Biffoni M, Todaro M, Invernici G, Cenci T, et al. Tumour vascularization via endothelial differentiation of glioblastoma stem-like cells. Nature. 2010; 468:824–8. [PubMed: 21102434]
38. Quintana E, Shackleton M, Sabel MS, Fullen DR, Johnson TM, Morrison SJ. Efficient tumour formation by single human melanoma cells. Nature. 2008; 456:593–8. [PubMed: 19052619]
39. Park DM, Rich JN. Biology of glioma cancer stem cells. Molecules and cells. 2009; 28:7–12. [PubMed: 19655094]
40. Li Y, Laterra J. Cancer stem cells: distinct entities or dynamically regulated phenotypes? Cancer research. 2012; 72:576–80. [PubMed: 22298594]
41. Kumar SM, Liu S, Lu H, Zhang H, Zhang PJ, Gimotty PA, et al. Acquired cancer stem cell phenotypes through Oct4-mediated dedifferentiation. Oncogene. 2012
42. Li Y, Li A, Glas M, Lal B, Ying M, Sang Y, et al. c-Met signaling induces a reprogramming network and supports the glioblastoma stem-like phenotype. Proceedings of the National Academy of Sciences of the United States of America. 2011; 108:9951–6. [PubMed: 21628563]
43. Reardon DA, Wen PY. Therapeutic advances in the treatment of glioblastoma: rationale and potential role of targeted agents. The oncologist. 2006; 11:152–64. [PubMed: 16476836]
44. Clarke MF, Becker MW. Stem cells: the real culprits in cancer? Scientific American. 2006; 295:52–9. [PubMed: 16830680]
45. Herlyn M, Villanueva J. Sorting through the many opportunities for melanoma therapy. Pigment cell & melanoma research. 2011; 24:975–7. [PubMed: 21899726]
46. Kirschmann DA, Seftor EA, Hardy KM, Seftor RE, Hendrix MJ. Molecular pathways: vasculogenic mimicry in tumor cells: diagnostic and therapeutic implications. Clin Cancer Res. 2012; 18:2726–32. [PubMed: 22474319]
47. Wang JY, Sun T, Zhao XL, Zhang SW, Zhang DF, Gu Q, et al. Functional significance of VEGF-a in human ovarian carcinoma: role in vasculogenic mimicry. Cancer biology & therapy. 2008; 7:758–66. [PubMed: 18376140]
48. Orgaz JL, Ladhani O, Hoek KS, Fernandez-Barral A, Mihic D, Aguilera O, et al. Loss of pigment epithelium-derived factor enables migration, invasion and metastatic spread of human melanoma. Oncogene. 2009; 28:4147–61. [PubMed: 19767774]
49. Strizzi L, Postovit LM, Margaryan NV, Lipavsky A, Gadiot J, Blank C, et al. Nodal as a biomarker for melanoma progression and a new therapeutic target for clinical intervention. Expert review of dermatology. 2009; 4:67–78. [PubMed: 19885369]
50. Hardy KM, Kirschmann DA, Seftor EA, Margaryan NV, Postovit LM, Strizzi L, et al. Regulation of the embryonic morphogen Nodal by Notch4 facilitates manifestation of the aggressive melanoma phenotype. Cancer research. 2010; 70:10340–50. [PubMed: 21159651]

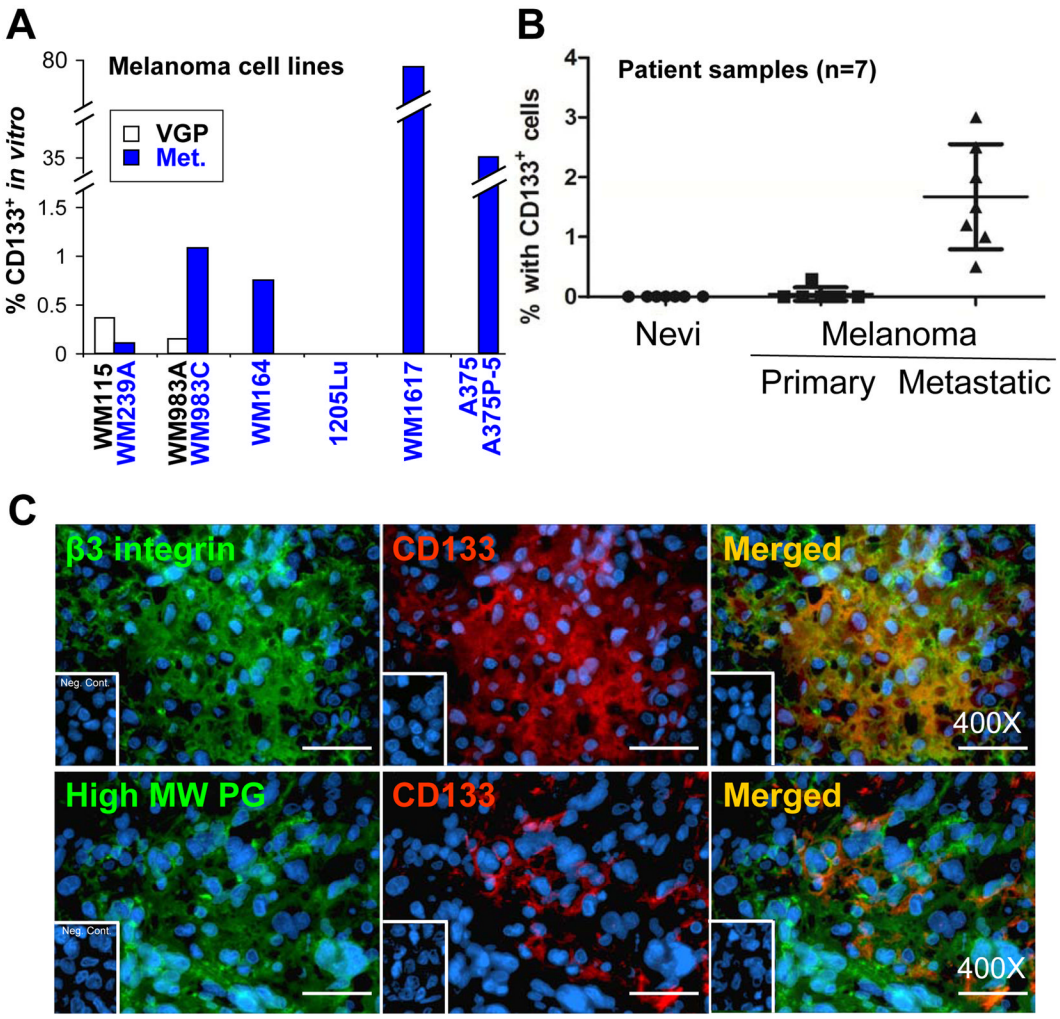

Figure 1.

Expression of CD133 subsets in melanoma. **A.** *In vitro* expression of CD133 in cultured melanoma cell lines was detected by PE-conjugated anti-CD133 (Miltenyi Biotec) using flow cytometry. □: Vertical growth phase (VGP) melanoma cell lines. ■: Metastatic melanoma (Met). **B.** CD133 expression in patient samples was examined by IF. Seven samples of each stage of melanoma progression were examined and the percentage of positive cells was recorded by examining 10 randomly chosen 400X fields. **C.** Double IF using antibodies directed to melanoma-associated antigen β3 integrin and high molecular weight proteoglycans (green, left panels) verified that the CD133-expressing cells (red, middle panels) in patient samples were indeed melanoma cells. Magnification: 400X; Scale bar, 25 μm.

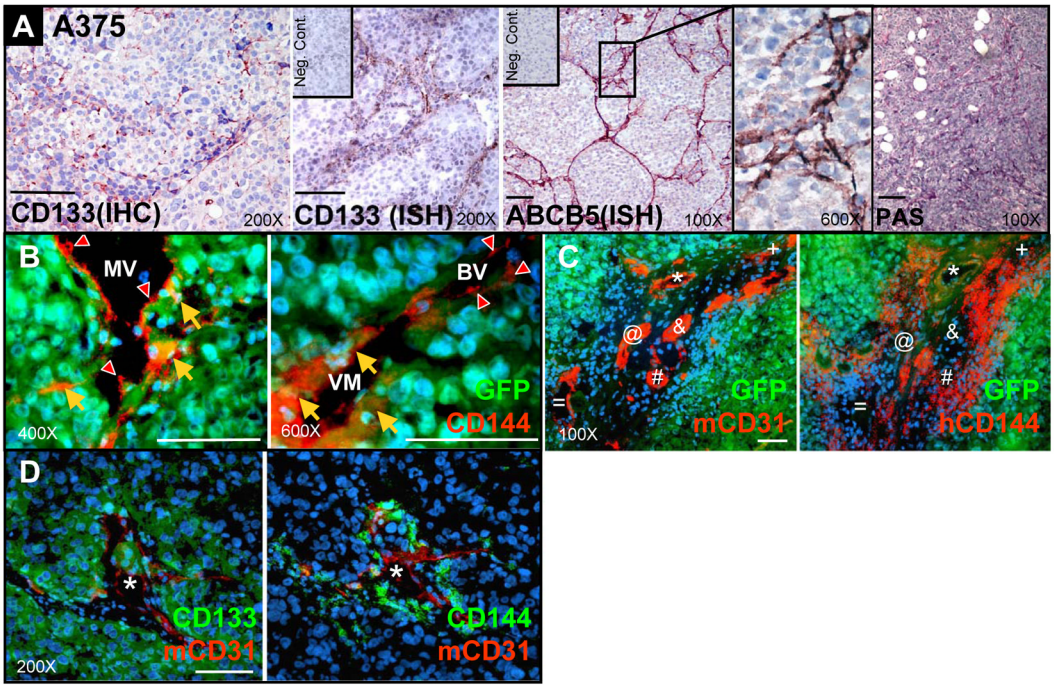

Figure 2.

Co-localization of CD133$^+$/ABCB5$^+$ subsets to CD144$^+$ VM areas. **A.** Immunohistochemistry for CD133 and *in situ* hybridization for CD133 and ABCB5 revealed branching network patterns identical to PAS$^+$ matrix-rich patterned network of VM in A375 melanoma xenografts. **B.** Double immunofluorescence in GFP-labeled A375 melanoma xenografts identifies circulatory networks consisting of CD144$^+$/GFP$^+$ VM channels (orange arrow), CD144$^+$/GFP$^-$ EC-lined authentic blood vessels (BV, red arrowhead), and mosaic vessels (MV) partially lined by both CD144$^+$/GFP$^+$ VM-engaging melanoma cells (orange arrow) and CD144$^+$/GFP$^-$ ECs (red arrowhead). **C.** In consecutive sections of GFP-labeled A375 melanoma xenografts, VM-engaging melanoma cells (hCD144$^+$/GFP$^+$ in orange; right panel) are in close physical proximity to high-density mouse blood vessels (mCD31$^+$ in red; left panel). Each symbol designates the same corresponding mouse blood vessel in consecutive sections. **D.** Double immunofluorescence localized the CD133$^+$ subsets (green, left panel) to the CD144$^+$ VM-engaging melanoma cells (green, right panel) surrounding the CD31$^+$ EC-lined blood vessel (red), the perivascular “niche” in consecutive sections of WM1617 xenograft. Each asterisk indicates the same corresponding blood vessel in both panels. Scale bar, 50 μm.

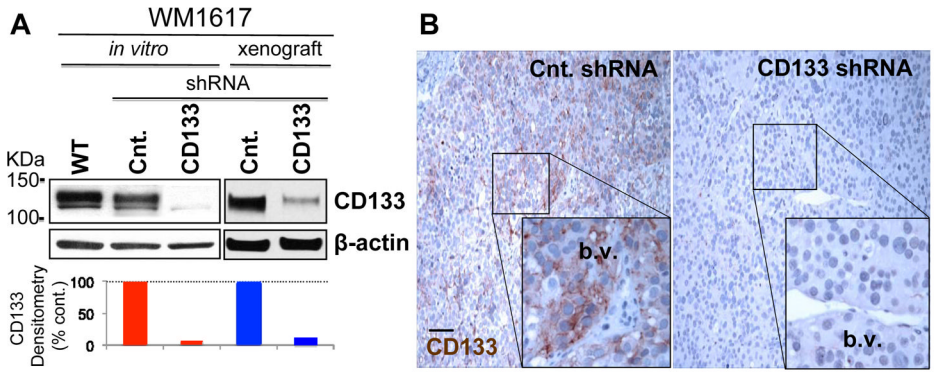

Figure 3.

CD133 silencing in melanoma using lentiviral shRNA. **A.** Cell lysates and xenograft homogenates prepared from WM1617 melanoma cells stably transfected with lentiviral shRNA against human CD133 and non-target control (Cnt.) were subjected to Western blotting. β-actin served as internal loading control. Greater than 90% CD133 KD efficiency was achieved *in vitro* and *in vivo* compared to the non-target control as determined by densitometry. WT: parental WM1617 non-transfectant. **B.** Immunohistochemistry confirmed CD133 silencing *in vivo* in WM1617 melanoma xenografts. Note that CD133 KD xenografts are devoid of CD133 expression, while those of non-target control retain constitutive CD133 expression in the perivascular "niche". b.v.: blood vessel. Magnification: 100X (Inserts: 400X); Scale bar, 50 μm.

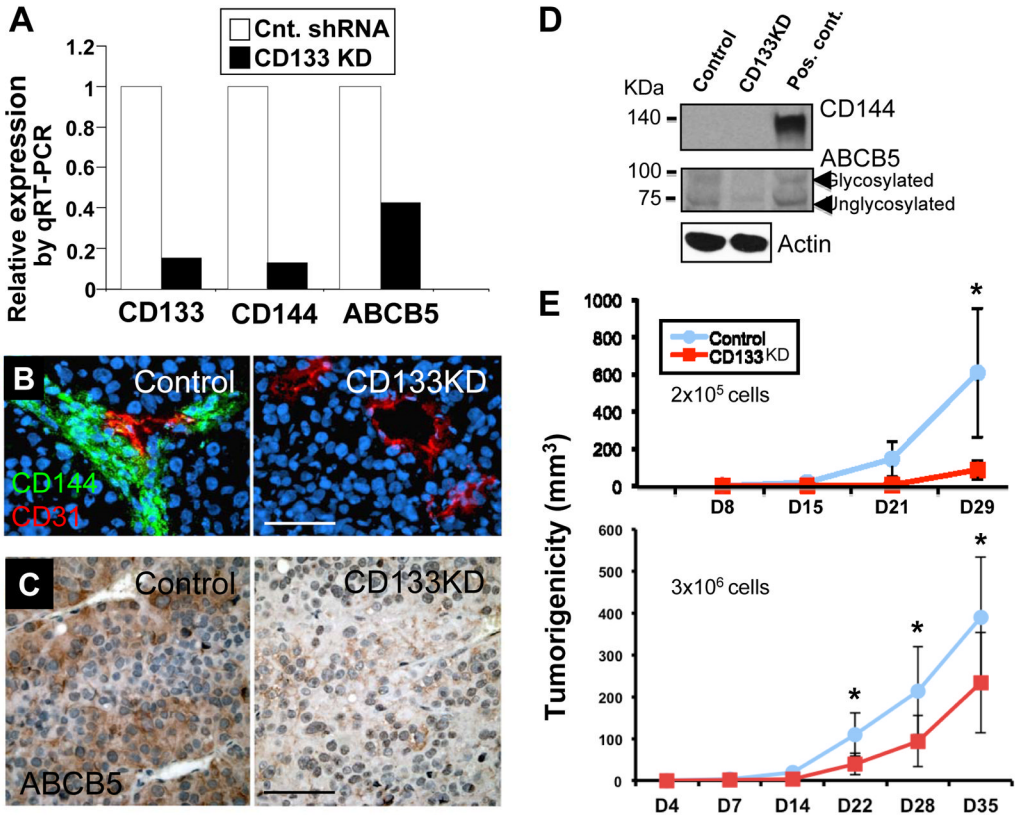

Figure 4.

Consequences of CD133 KD in WM1617 melanoma. **A.** Expression profiling by qRT-PCR revealed concomitant CD144 and ABCB5 downregulation in CD133 KD xenografts. □: non-target control. ■: CD133 KD. **B.** Immunofluorescence analysis showed attenuated $CD144^+$ VM-like channel formation in perivascular "niche" in CD133 KD xenografts. Magnification: 200X; Scale bar, 50 μm. **C.** Immunohistochemistry showed depletion of perivascular $ABCB5^+$ subsets in CD133 KD xenografts. Magnification: 200X; Scale bar, 50 μm. **D.** Western blotting for CD144 and ABCB5 expression in WM1617 xenografts. Unfortunately, despite maximal loading (40 μg protein per lane) and prolonged exposure (overnight), the expression of CD144 was under the detection limit both in the non-target control and in the CD133 KD xenografts (BAEC lysate was included as a positive control). On the other hand, ABCB5 downregulation in CD133 KD xenografts was confirmed by Western blotting (A375 cell lysate served as a positive control). **E.** Tumorigenicity assays revealed that CD133 KD in WM1617 melanoma cells resulted in significant growth inhibition *in vivo* (upper panel: n=5; 2×10^5 cells/mouse; lower panel: n=7; 3×10^6 cells/mouse). Asterisks indicate $p<0.05$.